Available online at www.sciencedirect.com
ScienceDirect
Acta Materialia 56 (2008) 5685–5693
Acta MATERIALIA
www.elsevier.com/locate/actamat

# Atomistic modeling of the interaction of glide dislocations with "weak" interfaces

J. Wang [a,*], R.G. Hoagland [a], J.P. Hirth [b], A. Misra [b]

[a] Materials Science and Technology Division, Los Alamos National Laboratory, Los Alamos, NM 87545, USA
[b] Center for Integrated Nanotechnologies, Materials Physics and Applications Division, Los Alamos National Laboratory, Los Alamos, NM 87545, USA

Received 1 July 2008; received in revised form 26 July 2008; accepted 26 July 2008
Available online 25 August 2008

**Abstract**

Using atomistic modeling and anisotropic elastic theory, the interaction of glide dislocations with interfaces in a model Cu–Nb system was explored. The incoherent Cu–Nb interfaces have relatively low shear strength and are referred to as "weak" interfaces. This work shows that such interfaces are very strong traps for glide dislocations and, thus, effective barriers for slip transmission. The key aspects of the glide dislocation–interface interactions are as follows. (i) The weak interface is readily sheared under the stress field of an impinging glide dislocation. (ii) The sheared interface generates an attractive force on the glide dislocation, leading to the absorption of dislocation in the interface. (iii) Upon entering the interface, the glide dislocation core readily spreads into an intricate pattern within the interface. Consequently, the glide dislocations in both Cu and Nb crystals are energetically favored to enter the interface when they are located within 1.5 nm from the interface. In addition to the trapping of dislocations in weak interfaces, this paper also discusses geometric factors such as the crystallographic discontinuity of slip systems across the Cu/Nb interfaces, which contribute to the difficulty of dislocation transmission across an interface. The implications of these findings to the unusually high strengths experimentally measured in Cu/Nb nanolayered composites are discussed.
Published by Elsevier Ltd on behalf of Acta Materialia Inc.

*Keywords:* Molecular dynamics; Dislocation; Interfaces; Multilayers; Slip transmission

## 1. Introduction

Nanoscale metallic multilayer composites exhibit relatively high flow strengths in comparison with bulk polycrystalline materials [1–8]. The flow strength of composite materials produced in this way is dependent on the thickness of the individual layers [1–14]. For individual layer thickness greater than ~50 nm, the dependence of strength on the layer thickness fits the Hall–Petch relation, implying that the predominant deformation mechanism involves dislocation pile-ups at the interfaces [4–6]. The effects of the discreteness of pile-ups on the layer thickness dependence of strength in multilayers have also been analyzed [9–13].

For layer thicknesses in the range of a few tens of nanometers, a model based on the confined layer glide of single dislocations was developed [6]. In this model, the interface barrier stress for single dislocation transmission is assumed to be greater than the confined layer slip stress and, hence, transmission of dislocation across the interfaces does not occur. The experimentally measured strength reaches a plateau at layer thicknesses below ~5 nm. As the confined layer slip stress is predicted to increase continuously with decreasing layer thickness, this suggests that the assumption of layer confinement of slip breaks down when the strength becomes sufficiently high and crossing of dislocations across interfaces becomes an important unit process at these length scales [6,13–22].

Earlier atomistic simulations performed by Hoagland et al. [16], showed that the peak strength of coherent Cu/Ni multilayers at layer thicknesses below ~5 nm may be interpreted in terms of the high coherency stresses that must be overcome for single dislocation transmission. However, in the incoherent Cu/Nb system, direct transmission of glide

* Corresponding author. Tel.: +1 505 667 1238.
*E-mail address:* wangj6@lanl.gov (J. Wang).

1359-6454/$34.00 Published by Elsevier Ltd on behalf of Acta Materialia Inc.
doi:10.1016/j.actamat.2008.07.041

dislocations was not observed at reasonable values of applied stress in atomistic model [17,18], indicating that these interfaces present an unusually strong barrier for slip transmission. This paper describes results that provide additional insight into how interfaces act as barriers for single dislocation transmission across interfaces. Several important issues are examined in detail, such as interface structures, interface properties and glide dislocation–interface interactions.

Using atomistic modeling, Cu and Nb crystals are assembled into a bilayer with the Kurdjumov–Sachs (KS) crystallographic orientation relation. This epitaxy is observed in experiments on this multilayer composite. It corresponds to the $\{111\}_{Cu}\|\{110\}_{Nb}\|$ interface plane and $\langle 1\,10\rangle_{Cu}\|\langle 1\,11\rangle_{Nb}$ in the interface plane. Previous work on this system revealed that the atomic structures of Cu/Nb interfaces could have multiple states [18–22]. Three possible atomic structures of Cu/Nb interfaces with nearly degenerate energies are identified. The interface formation energy and areal density of atoms in these interfaces are summarized in Table 1. The atomic structure referred to as $KS_1$ is formed by directly combining two semi-infinite perfect crystals according to the KS orientation relation [18,19]. Another, referred to as $KS_2$, is formed by inserting a strained monolayer of Cu{111} as an intermediate layer between the adjoining crystals in the $KS_1$ interface [20]. One can create this inserted monolayer, denoted as $Cu^{\alpha}$, by straining a perfect Cu{111} monolayer in the manner described in Ref. [20]. Consequently, two interfaces form, referred to as $Cu/Cu^{\alpha}$ and $Cu^{\alpha}/Nb$. A third structure, referred to as $KS_{min}$, is formed by removing some atoms in the first Cu layer from either $KS_1$ or $KS_2$ to reach a minimum in the interface formation energy [18].

The shear resistance and sliding mechanisms of Cu–Nb interfaces (in the absence of any lattice glide dislocations in the vicinity of the interface) have been reported in recent work [18,21,22]. Simulation results revealed that the shear strengths of Cu/Nb interfaces are: (i) significantly lower than the theoretical estimates of shear strengths for slip planes in perfect crystals of Cu and Nb; (ii) spatially non-uniform within interfaces; (iii) strongly dependent on the atomic structures of the interfaces, with $KS_2$ the weakest and $KS_{min}$ the strongest; and (iv) strongly dependent on the applied in-plane shear direction. The mechanisms of interface sliding involve nucleation and glide of interfacial dislocation loops that nucleate in the weakest regions of the interfaces.

This work focuses on the interaction of glide dislocations with the Cu/Nb interfaces to gain insight into how interfaces act as barriers for slip transmission. Atomistic simulations and anisotropic elastic analysis are carried out to investigate the interaction of lattice glide dislocations with the three types of Cu/Nb interfaces ($KS_1$, $KS_2$, and $KS_{min}$). Simulation details are elaborated in Section 2, and the results are summarized and discussed in Section 3. Finally, conclusions are drawn in Section 4.

## 2. Methodology of atomistic simulations

A rectangular bilayer model composed of Cu and Nb crystals with a periodic boundary condition along the $z$ axis is adopted. The bilayer model is rectangular in shape and divided into a two-part computational cell, as shown in Fig. 1. One part, region 1, contains moveable atoms embedded in a semi-rigid part, region 2. According to the KS orientation relation, the bilayer model has $[1\bar{1}2]_{Cu}$ parallel to $[1\bar{1}2]_{Nb}$, $[111]_{Cu}$ parallel to $[110]_{Nb}$, and $[1\bar{1}0]_{Cu}$ par-

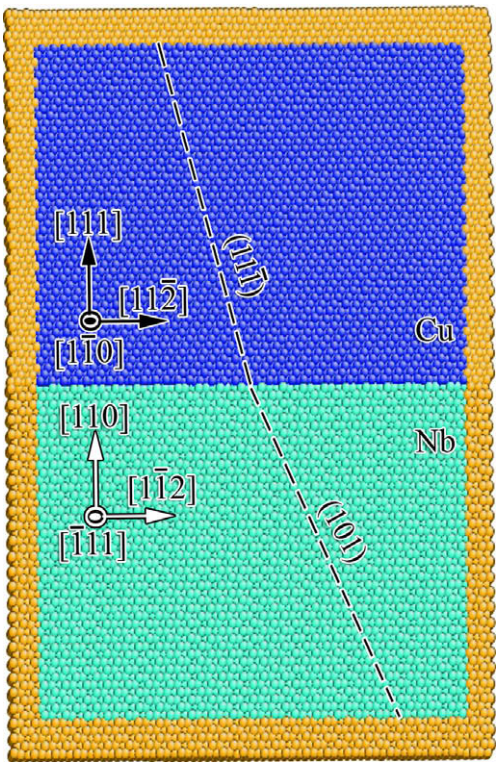


Fig. 1. Simulation cell of the rectangle bilayer, showing region 1 – the moveable part containing Cu atoms in the upper crystal and Nb atoms in the lower crystal – colored in shades of blue, and region 2 – the semi-rigid part – (see text) colored yellow. Two slip planes are denoted as dashed lines: $(11\bar{1})_{Cu}$ and $(101)_{Nb}$. The $x$ axis lies along $[11\bar{2}]_{Cu}$, the $y$ axis along $[111]_{Cu}$, and the $z$ axis along $[1\bar{1}0]_{Cu}$. The thickness along the $z$ axis is ~4.86 nm. The dimension in region 1 is 16 nm along the $x$ axis, and the height along the $y$ axis is 16 nm for each crystal. (For interpretation of color mentioned in this figure the reader is referred to the web version of the article.)

Table 1
Interface energies and areal densities of the interfacial Cu plane of (111)Cu/(110)Nb interface in three different atomic arrangements: $KS_1$, $KS_2$, and $KS_{min}$

| Configuration | Interface energy ($J\,m^{-2}$) | Areal density of interfacial Cu plane (atoms $nm^{-2}$) |
|---|---|---|
| $KS_1$ | 0.5687 | 17.74 |
| $KS_2$ | 0.5675 | 17.58 |
| $KS_{min}$ | 0.5414 | 16.82 |

allel to $[\bar{1}11]_{Nb}$. The *xyz* coordinate system is chosen as shown in Fig. 1. The dimensions of the simulation cell are ~18.6 nm in the *x* direction, 4.86 nm in the *z* direction, and 18.6 nm in the *y* direction for both Cu and Nb crystals. These dimensions take advantage of the quasiperiodicity that exists in the interface as described in Ref. [21].

The equilibrium, 0 K, structures are obtained via relaxation by quenching molecular dynamics, as described in Ref. [19]. Embedded atom method (EAM) potentials are used for Cu [23] and Nb [24]. These potentials have produced good results for surface diffusion and defect formation energies [25–27]. As no significant ionic or directional covalent bonding is expected to be present between Cu and Nb, the interaction potentials designed to model bonding between these two elements are based on the usual form used for other metal pairs [28], and the construction of EAM interaction potentials for pairs of metal elements is typically accomplished by fitting the corresponding values of dilute enthalpies of mixing [29] and/or the experimentally determined properties of intermetallic phases formed by these elements [30]. Since the immiscible CuNb system does not posses any intermetallic phases, however, the interaction potentials were instead constructed based on the dilute enthalpies of mixing obtained from analytical fitting of the CuNb phase diagram [31] as well as the lattice constant and bulk modulus of a hypothetical CuNb crystal in the CsCl structure obtained by first-principles calculations using VASP [32]. Because EAM potentials are especially capable of capturing the dependence of atom energies on atom coordination [33], the excess fitting parameters are used in this study to construct potentials with differing average cohesive energies $E_{coh}$ of CuNb in the NaCl structure, the ZnS structure and a single sheet of the BN structure [20]. This potential has been used to model the atomic structures of Cu/Nb interfaces [16–22,34] and the growth mechanisms of Cu/Nb layered composites during physical vapor deposition [35]. During the relaxation, the two crystals are able to undergo relative translation in three directions, but rotation is not allowed. The net forces, acting parallel and perpendicular to the interface, drive the translations [18,21,22].

Lattice glide dislocations are introduced in the bilayer model by the application of the anisotropic Barnett–Lothe solutions [36] for the displacement field of a dislocation at an interface between two elastically dissimilar materials. This field is applied to both the moveable and the fixed regions of the bilayer model. The dislocation line is parallel to the *z* axis in all cases. Relaxations of the model containing dislocations are accomplished by quenching molecular dynamics until the maximum force acting on any atom in the system does not exceed 5 pN.

When a lattice glide dislocation enters the interface, disregistry analysis is carried out to determine slip in the interface that is sheared by the dislocation stress field [18,21,22]. In this analysis, pairs of atoms that straddle the desired shear plane are first identified in a reference, relaxed system. The vector $\vec{r}_{ij}$ describes the relative position, $\vec{r}_{ij} = \vec{r}_i - \vec{r}_j$, between the *i*th atom and the *j*th atom that forms a pair in the reference, relaxed system, where the vector $\vec{r}_i$ describes the position of the *i*th atom in the reference system. The displacements of these atoms in the sheared system are determined with respect to the reference system. The vector $\vec{r}^{\,d}_{ij}$ describes the relative position, $\vec{r}^{\,d}_{ij} = \vec{r}^{\,d}_{ij} - \vec{r}_{ij}$, between the *i*th atom and the *j*th atom in the sheared system, where the vector $\vec{r}^{\,d}_i$ describes the position of the *i*th atom in the sheared system. The disregistry vector is calculated as the difference of the two vectors, $\vec{r}_{ij} - \vec{r}_{ij}$.

## 3. Interaction of lattice glide dislocations with interfaces

### 3.1. Slip systems in Cu/Nb

The active slip systems for a layered Cu/Nb geometry subjected to either compressive stress normal to the interface plane or tensile stress parallel to the interface plane are considered. In these two situations, there is no resolved shear stress on the glide planes that make up the interface plane. There are three {1 1 1} planes in Cu and five {1 1 0} planes in Nb that are non-parallel to the interface plane and, hence, have finite resolved shear stress for uniaxial loading normal or parallel to the interface. Several important features are summarized here. First, the active slip planes in Cu and Nb are not parallel. Second, only one set of {1 1 1}Cu and {1 1 0}Nb glide planes have a common trace of intersection in the interface plane, as shown in Fig. 2. For other planes, the dislocation lines are not parallel when dislocations enter the interface from the Cu and Nb crystals. Finally, the Burgers lengths of dislocations in Cu and Nb crystals are different: 0.2556 nm for dislocations in Cu crystal and 0.2858 nm for dislocations in Nb crystal. Slip discontinuity in the Cu/Nb layered composites makes dislocation transmission particularly difficult.

The interactions of lattice glide dislocations on the eight conventional slip planes (three in Cu and five in Nb) with the three atomic structures of Cu/Nb interface were systematically investigated. However, this paper focuses on the results of the interaction of three types of interfaces with lattice glide dislocations on planes that have a common trace of intersection with the interface, Cu $(11\bar{1})$ and Nb (1 0 1), marked in Fig. 1. The interactions of lattice glide dislocations on the other six conventional glide planes with interfaces, studied with a three-dimensional bilayer model, are discussed.

### 3.2. Core spreading of lattice glide dislocation within interfaces

A single full dislocation consisting of two Shockley partials is introduced in the Cu crystal of the bilayer model. The two partials connected by a stacking fault are initially separated by 2.5 nm, which is the equilibrium distance for two partials under zero applied stress for this Cu potential,

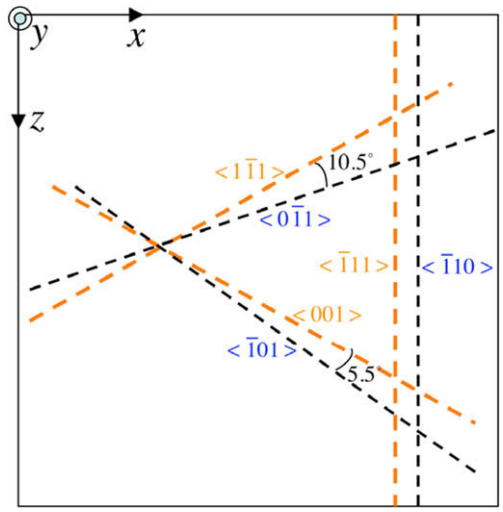


Fig. 2. Traces of intersections of {1 1 1}Cu and {1 1 0}Nb slip planes with the interface. Three black dashed lines, parallel to Cu ⟨1 1 0⟩, represent intersections of interface plane with the three {1 1 1}Cu slip planes. Three orange dashed lines represent intersections of the interface plane with {1 1 0}Nb slip planes. The $z$ axis in the bilayer model is parallel to Cu [1̄10] and Nb [1̄11]. (For interpretation of color mentioned in this figure the reader is referred to the web version of the article.)

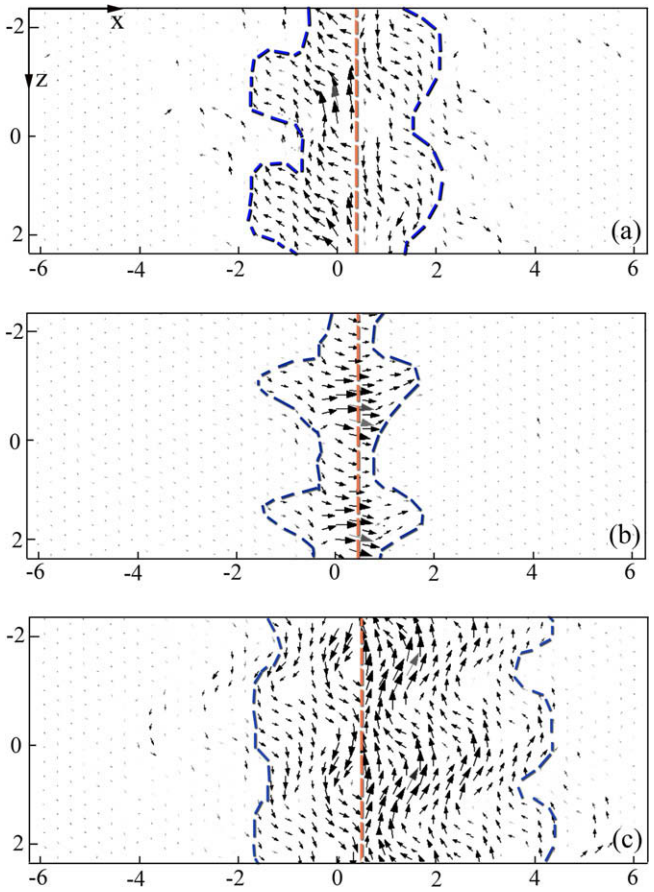


Fig. 3. Patterns in the vector field plots of disregistry across the interface plane, showing core spreading for (a) an edge Shockley partial, (b) a mixed Shockley partial, and (c) a perfect screw dislocation entering the $KS_1$ interface from the Cu crystal. The horizontal axis is along the $x$ direction, and the vertical axis along the $z$ direction in the bilayer model. The length unit is nanometers in both axes. The arrows represent magnitudes and directions of disregistry vectors. The orange dashed line indicates the intersection of the slip plane with the interface. The blue dashed lines separate the slipped regions from the non-slipped regions.

and the leading partial is at a distance of 1.5 nm from the interface. Three types of full dislocations are studied: one screw dislocation and two mixed dislocations with different leading Shockley partials, mixed or edge partial. Relaxations are accomplished by quenching molecular dynamics under zero applied stress. The results reveal that the leading Shockley partial, no matter what type or sign, spontaneously enters the interface, behavior associated with core spreading within the interface. With increased applied stress, dislocation transmission from Cu to Nb does not occur, even with the resolved shear stress in Nb as high as 1.6 GPa. Figs. 3–5 show the disregistry plots of lattice glide dislocations in the interface planes for $KS_1$, $KS_2$, and $KS_{min}$, respectively. The arrowed lines represent disregistry vectors, showing the directions and magnitudes of slip within an interface; the dashed curves outline the boundary between the slipped region and the non-slipped region within the interface.

The cores of lattice glide dislocations readily spread into intricate patterns within interfaces. This feature is ascribed to spatial non-uniformity of interfacial shear resistance [21]. Owing to the low interfacial shear resistance, the width of the spread core of an edge partial in the $KS_1$ interface is ~4 nm, as shown in Fig. 3a, more than 15 times the Burgers length.

Core spreading is accompanied by the local rearrangement of atoms within the interface. As shown in Fig. 3a, although the in-plane component of the Burgers vector of an edge partial is along the $x$ direction, the disregistry vectors identifying the shear that has occurred are not parallel to this direction.

Both mixed Shockley partials associated with a perfect screw dislocation enter the interface under zero applied stress, accompanied by core spreading within interfaces (Figs. 3c and 4). As a result, a screw dislocation initially gliding on Cu (1 1 1) crosses slips onto the interface plane. For a dissociated mixed dislocation, the leading partial enters the interface as a consequence of core spreading within the interface, but the trailing Shockley partial remains standing off from the interface.

The dislocation core spreads only in the Cu–Nb interface for the $KS_1$ (Fig. 3) and $KS_{min}$ interfaces (Fig. 4c), but spreads in two interface planes, Cu–$Cu^{\alpha}$ and $Cu^{\alpha}$–Nb for $KS_2$, as shown in Fig. 4a and b.

The extent of core spreading within the interfaces depends on their atomic structures. Core spreading is much larger in magnitude in the $KS_2$ interface than in the other two types of interfaces, as shown in Figs. 3 and 4, consistent with the fact that $KS_2$ interface has the lowest shear resistance [21].

Similar features are observed for the interaction of glide dislocations in the Nb crystal with the interfaces. Two types of dislocations, screw and mixed, are introduced in

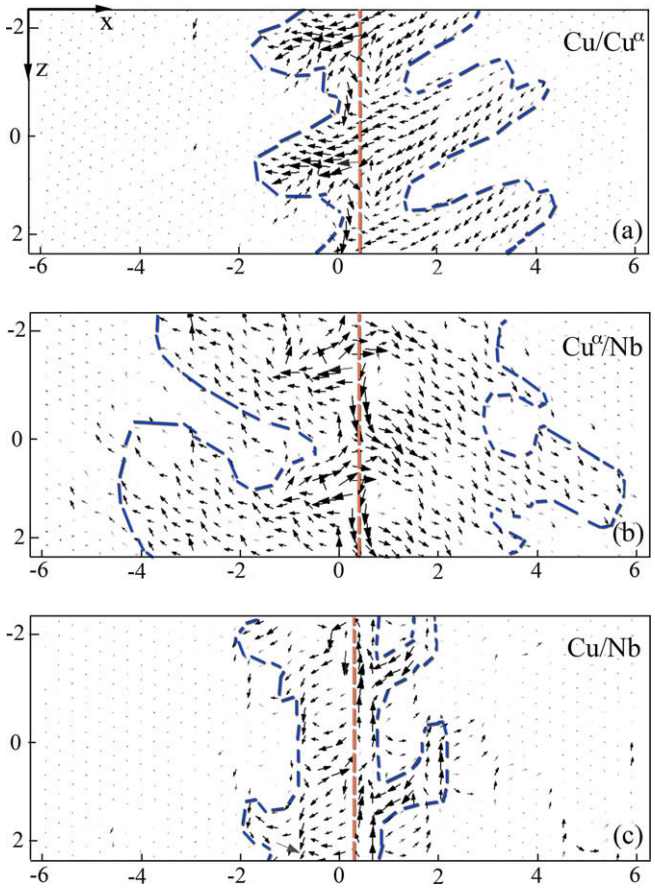


Fig. 4. Patterns in the vector field plots of disregistry across the interface plane, showing core spreading in two interface planes, (a) Cu/Cu$^{\alpha}$ and (b) Cu$^{\alpha}$/Nb as an edge Shockley partial enters the $KS_2$ interface from the Cu crystal, and (c) in the Cu/Nb interface as an edge Shockley partial enters the $KS_{min}$ interface from Cu crystal. The horizontal axis is along the $x$ direction, and the vertical axis along the $z$ direction in the bilayer model. The length unit is nanometers for both axes. The arrows represent magnitudes and directions of disregistry vectors. The orange dashed line indicates the intersection of slip plane with the interface. The blue dashed lines separate the slipped regions from the non-slipped regions.

the Nb crystal of the bilayer model, initially located at 1.5 nm from the interface. Under zero applied stress, both types of dislocations, no matter what sign, spontaneously enter the interface, as a consequence of core spreading. Fig. 5 shows the disregistry plots of core spreading of a screw dislocation and a mixed dislocation within the $KS_1$ interface. The region of core spreading is wider for a screw dislocation than for a mixed dislocation. One important difference from the result for dislocations in Cu is that a mixed dislocation initially in Nb can dissociate into the Cu crystal, emitting a Shockley partial dislocation near the trace of the Nb slip plane on the interface when the applied tensile stress is 1 GPa. Fig. 6 shows the dissociation of a mixed dislocation in Nb when it enters the interface. However, it is noticed that slip transmission is still difficult, because the partial dislocations cannot move away from the interface until the resolved shear stress is increased to unreasonably high values in excess of 1.10 GPa.

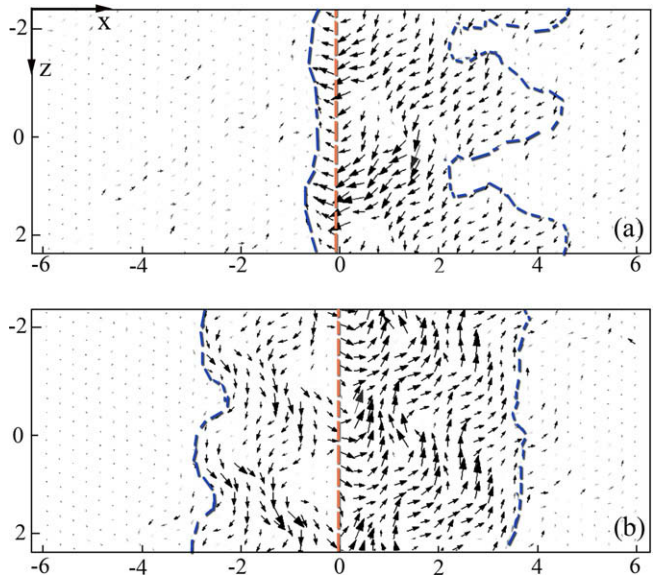


Fig. 5. Patterns in the vector field plots of disregistry across interface plane, showing core spreading as (a) a mixed dislocation and (b) a screw dislocation enters the $KS_1$ interface from the Nb crystal. The horizontal axis is along the $x$ direction, and the vertical axis along the $z$ direction in the bilayer model. The length unit is nm for both axes. The arrows represent magnitudes and directions of disregistry vectors. The orange dashed line indicates the intersection of slip plane with the interface. The blue dashed lines separate the slipped regions from the non-slipped regions.

### 3.3. Sheared interface attracts lattice glide dislocation

Owing to the lower shear resistance of interfaces, the interface can be sheared under the stress field of the glide dislocation when the dislocation approaches the interface. As a consequence, the sheared interface generates an attractive force on the lattice glide dislocation. To provide an estimate of the strength of the attraction force, Hoagland et al. [18] developed an analytical model using a dislocation approach, in which the sheared interface is described by sets of virtual dislocations. It has been shown that the extent of the shear occurring in the interface is determined by the spatial variation in interface shear resistance, which was not incorporated in the analytical model.

Using the atomistic model and theoretical analysis, the energetics of glide dislocations as they move towards interfaces are computed. Owing to the elastic mismatch between Cu and Nb crystals, lattice glide dislocations are acted on by the Koehler force, either attractive or repulsive, which depends on the variation in line energy of a dislocation with respect to its location in a crystal or at an interface [36,37]. As derived by Barnett and Lothe for dislocations in anisotropic bicrystals [36], the Koehler force normal to the interface plane for a dislocation situated at a distance $h$ from the interface can be written in a simple form: $f_k = (E^{\infty} - E^{1-2})/h$. Here, $E^{\infty}$ is the prelogarithmic energy factor of the line energy of the same dislocation in an infinite homogeneous medium elastically identical to the half space in which it resides, and $E^{1-2}$ is the prelogarithmic

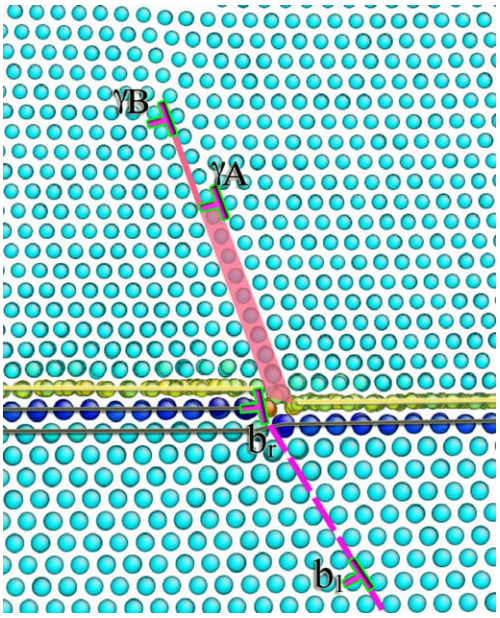


Fig. 6. Dissociation of a mixed dislocation in the Nb crystal (blue atoms below) into the Cu crystal (cyan atoms above). Two Shockley partials are emitted near the trace of the Nb slip, and trail an extrinsic stacking fault in the Cu crystal (marked as a thick solid line). $b_1$ represents a mixed dislocation with Burgers vector (−0.1348, 0.2334, and −0.0954) nm in the model coordinate initially situated at a distance of 1.5 nm from the interface. $\gamma^A$and $\gamma^B$ are mixed Shockley partial dislocations with Burgers vectors (−0.0246, 0.0696, and 0.1278) nm and (−0.0246, 0.0696, and −0.1278) nm in the model coordinate, respectively. $b_r$ is residual, sessile dislocation in the interface with Burgers vector (−0.0856, 0.0942, and −0.0954) nm in the model coordinate. (For interpretation of color mentioned in this figure the reader is referred to the web version of the article.)

factor of line energy of the same dislocation located at the interface of the bicrystal. The prelogarithmic energy factor of lattice glide dislocations is calculated when they are located in the Cu crystal, in the Nb crystal and in the interface. The results are listed in Table 2, and reveal that a dislocation has the lowest line energy when it is in Nb. Therefore, the glide of lattice dislocations in Cu crystal towards the interface is energetically favorable but, from the standpoint of Koehler force, the glide of a dislocation in Nb crystal towards the interface is not energetically favorable. However, atomistic simulations indicate that lattice dislocations in Nb crystal can spontaneously glide towards the interface when the initial distance from interface is <1.5 nm. This suggests that a critical distance exists for dislocations in Nb crystal moving towards interfaces. When the distance is larger than the critical distance, a dislocation is repelled from the interface, whereas the force is attractive for distances less than critical, and this attraction derives from shearing the interface.

In order to quantify the critical distance, the relative potential energy associated with a glide dislocation approaching the interface is calculated as a function of the distance between the dislocation and the interface. Two parts of the energy, one arising from the Koehler force and the other from the sheared interface, are considered.

Table 2
Prelogarithmic energy factors of the line energies of a dislocation situating in crystal or at the interface (ev nm$^{-1}$)*

| Dislocation | $E^{\infty}_{Cu}$ | $E^{\infty}_{Nb}$ | $E^{1-2}$ | $E^{\infty}_{Cu} - E^{1-2}$ | $E^{\infty}_{Nb} - E^{1-2}$ |
|---|---|---|---|---|---|
| Mixed in Cu crystal | 2.475 | | 2.092 | **0.383** | |
| Screw in Cu crystal | 1.547 | | 1.491 | **0.056** | |
| Mixed in Nb crystal | | 2.368 | 2.777 | | **−0.409** |
| Screw in Nb crystal | | 1.799 | 1.864 | | **−0.065** |

* In the bilayer model, the Burgers vector of the mixed dislocation in Cu is (0.0738, −0.2087, and 0.1278) nm or (0.0738, −0.2087, and −0.1278) nm on slip plane Cu $(11\bar{1})$; the Burgers vector of the screw dislocation in Cu is (0, 0, and 0.2556) nm on glide plane Cu $(11\bar{1})$; the Burgers vector of the mixed dislocation in Nb is (−0.1348, 0.2334, and −0.0954) nm on glide plane Nb (101) and (0, 0, and 0.2858) nm for screw dislocation in Nb.

The Koehler force acting on glide dislocations is computed from the anisotropic solution [36], and then the relative potential energy due to the Koehler force is integrated as a function of the distance between the dislocation and the interface. As shown in Fig. 7, the relative potential energy always decreases for lattice glide dislocations in Cu, but increases for lattice glide dislocations in Nb, with decreasing distance.

As the core of the lattice glide dislocation spreads into a complicated pattern within the interface, the relative potential energy due to the interface shear is determined from atomistic simulations as a function of the distance between the dislocation and the interface. A lattice glide dislocation is initially introduced in the bilayer model, located at a distance $h$ from the interface. This configuration containing a lattice glide dislocation is then relaxed under two different constraint conditions. One is to relax this configuration fully without any constraint, and the corresponding final potential energy is $E^f(h)$; the second is to relax this configuration while fixing atoms within the interface, and the corresponding final potential energy is $E^{\text{fix}}(h)$. The relative potential energy $E^I(h)$ is computed as the energy difference $E^f(h)$–$E^{\text{fix}}(h)$, corresponding to the contribution of the sheared interface to the total potential energy of the simulated system.

As shown in Fig. 7, the relative potential energy arising from interface shear decreases with distance below 4 nm, indicating the onset of interface shear. The total relative potential energy, consisting of two parts due to Koehler force and due to the sheared interface, is plotted in Fig. 7. For glide dislocations in Cu crystal, the potential energy always decreases as a glide dislocation approaches the interface. For glide dislocations in Nb, the potential energy increases until a critical distance is reached, and then decreases. The influence of interface structure ($KS_1$, $KS_2$, and $KS_{min}$) on the energy of a system containing a mixed dislocation in Nb approaching the interface is shown in Fig. 8. Fig. 9 shows the potential energy as a function of the distance for different types of dislocations moving towards the $KS_1$ interface, to reveal the influence of the force exerted by the sheared interface on different dislocation types. Several important features are as follows.

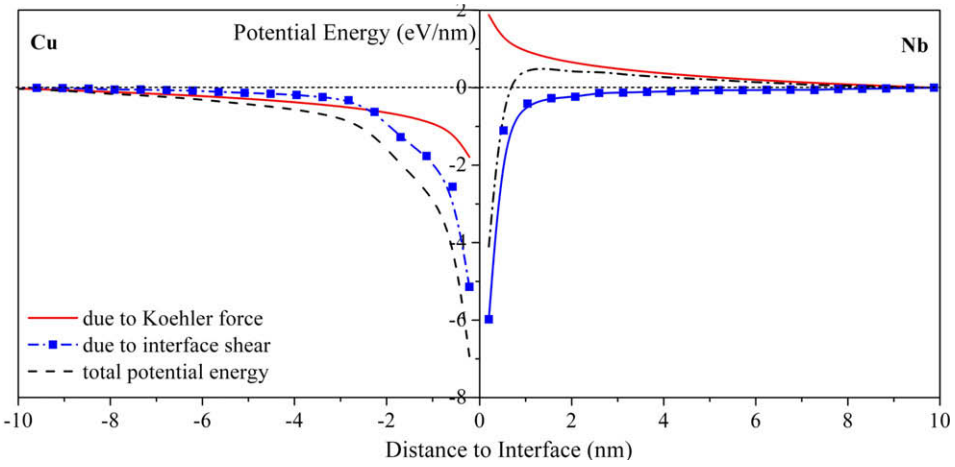


Fig. 7. The potential energies associated with a mixed dislocation approaching the $KS_1$ interface, (left) a mixed dislocation with Burgers vector (0.0738, −0.2087, and 0.1278) nm in the Cu crystal, and (right) a mixed dislocation with Burgers vector (−0.1348, 0.2334, and −0.0954) nm in the Nb crystal. The red solid lines represent the potential energy due to the Koehler force, the blue curves describe the relative potential energy due to interface shear, and the total potential energy in a dashed black curve. (For interpretation of color mentioned in this figure the reader is referred to the web version of the article.)

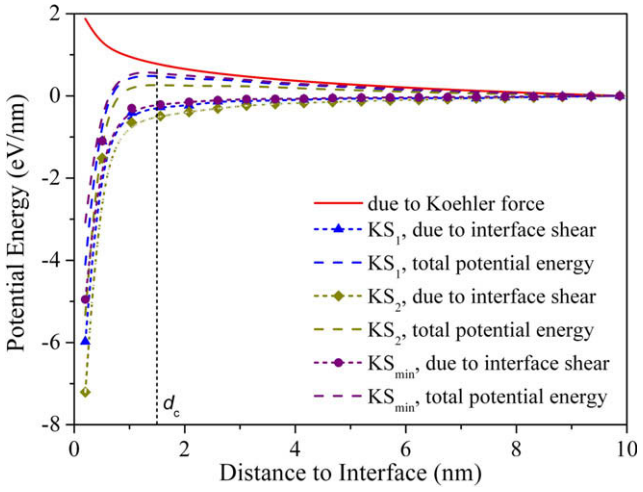


Fig. 8. The potential energies associated with a mixed dislocation with Burgers vector (−0.1348, 0.2334, and −0.0954) nm in the Nb crystal approaching interfaces: $KS_1$, $KS_2$, and $KS_{min}$. $d_c$ is the critical distance below which the dislocation experiences an attractive force. The red solid lines represent the potential energy due to the Koehler force, the blue curves describe the relative potential energies due to interface shear, and the total potential energies are shown in dashed curves. (For interpretation of color mentioned in this figure the reader is referred to the web version of the article.)

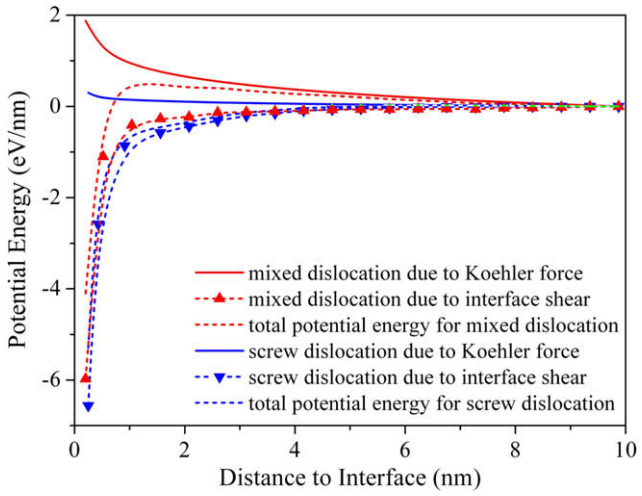


Fig. 9. The potential energies associated with a mixed dislocation with Burgers vector (−0.1348, 0.2334, and −0.0954) nm in the Nb crystal and a screw dislocation with Burgers vector (0, 0, and 0.2858) nm in the Nb crystal approaching the $KS_1$ interface. Red curves represent potential energies for a mixed dislocation, and blue curves describe potential energies for a screw dislocation. (For interpretation of color mentioned in this figure the reader is referred to the web version of the article.)

The total potential energy always decreases for a Cu glide dislocation approaching the interface.

The total potential energy associated with a glide dislocation in Nb approaching the interface initially increases owing to Koehler force repulsion, and then decreases below a critical distance when the interface begins to shear and the net force on the dislocation becomes attractive.

The critical distance at which the first derivative of the total relative potential energy with respect to the distance is zero in Nb is ~1.5 nm for the $KS_{min}$ interface, 1.56 nm for the $KS_1$ interface, and 1.68 nm for the $KS_2$ interface. The differences of the critical distances are ascribed to the different interfacial shear resistances, the strongest being the $KS_{min}$ interface and the weakest the $KS_2$ interface. More importantly, the occurrence of this critical distance suggests that dislocations cannot stay in an Nb layer if the thickness of the Nb layer is <3 nm. This result is in agreement with experimental observations. Transmission electron microscopy (TEM) studies on cold-rolled Cu–Nb multilayers showed that the films exhibit large plastic deformation without dislocation cell structure formation inside layers [38]. Also, TEM studies of as-synthesized Cu–Nb nanolayers [6] do not show dislocations parallel to the interfaces at some standoff distance.

Screw dislocations are subjected to a larger attractive force than mixed dislocations. As shown in Fig. 9, the relative potential energy due to the Koehler force is smaller for a screw dislocation than for a mixed dislocation in the Nb crystal. In addition, the slipped region of the interface is wider when a screw dislocation enters the interface than when a mixed dislocation does (Figs. 3 and 4).

As a consequence, the attractive force traps the dislocation that was absorbed into the interface, thereby increasing the applied force needed for dislocations to move away from the interface. Trapping is somewhat more effective in the $KS_2$ interface than in the $KS_1$ interface, because the $KS_2$ interface has the lowest shear resistance among the three types of interfaces. For example, a mixed dislocation in a Cu crystal, after entering the $KS_1$ interface, cannot be drawn back into the Cu crystal until the resolved shear stress reaches 0.95 GPa. The applied tensile stress must reach 1.10 GPa for a mixed dislocation in the $KS_2$ interface, because this interface is sheared more easily than the $KS_1$ interface.

### *3.4. Core spreading is a generic feature within weak interfaces*

Using a three-dimensional bilayer model, the authors investigated interactions of lattice glide dislocations on another six conventional glide planes with different types of interfaces. The results reveal the same features as mentioned in Sections 3.2 and 3.3. Lattice glide dislocations spontaneously enter the interfaces when introduced at a distance <1.5 nm, accompanied by interface shear and core spreading within the interfaces.

With several dislocations within an interface, interactions between them can augment core spreading. Fig. 10 shows the disregistry plots for the $KS_1$ interface, with the dashed lines separating slipped regions and non-slipped regions for the case where two identical edge Shockley partial dislocations entered the interface with a separation of 0.155 nm. The extent of core spreading for the two dislocations is confined only to the region between the two dislocations. Other combinations of dislocations within interfaces were examined but are not described here. The important result of this study is that core spreading is a generic feature due to the low interfacial shear resistance, regardless of the types and signs of dislocations, the active slip planes, and the dislocation combinations in the interface. As a result, the low interfacial shear resistance is essential for trapping dislocations, which in turn is important in providing a strong barrier to slip transmission, particularly in the absence of the mechanical advantage of a pile-up, and therefore, high strength in nanolayered composites.

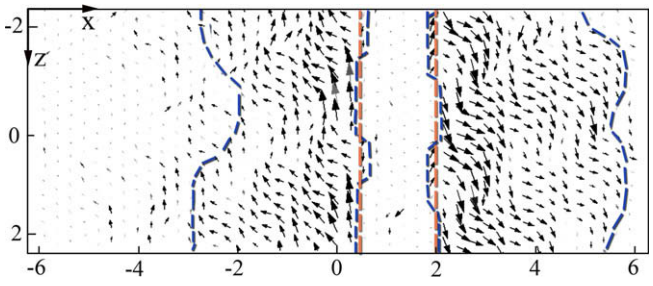


Fig. 10. Patterns in the vector field plots of disregistry across the interface plane, showing core spreading when two identical edge Shockley partial dislocations with a separation of 1.55 nm enter the $KS_1$ interface. The horizontal axis is along the $x$ direction, and the vertical axis along the $z$ direction in the bilayer model. The length unit is nm for both axes. The arrows represent magnitudes and directions of disregistry vectors. The orange dashed line indicates the intersection of slip plane with the interface. The blue dashed lines separate the slipped regions from the non-slipped regions. (For interpretation of color mentioned in this figure the reader is referred to the web version of the article.)

## 4. Summary and discussion

Cu/Nb multilayer composites reach peak strength when the individual layer thickness is reduced to a few nanometers. In this size regime, single dislocation transmission across the interface, unaided by a pile-up, becomes the critical unit process. Using atomistic modeling and anisotropic elastic theory, it was demonstrated that interfaces act as strong barriers for slip transmission. In addition to the geometric factor of slip discontinuity in Cu/Nb layered composites, the results reveal several important factors, directly related to the weak interfaces that hinder dislocation transmission across interfaces.

First, interfaces are readily sheared under the stress field of a glide dislocation owing to the low interfacial shear resistance. Second, the sheared interfaces generate an attractive force on the glide lattice dislocation, trapping the glide dislocation within interfaces. Third, the core of a glide lattice dislocation readily spreads into an intricate pattern owing to the low interfacial shear resistance and the spatial non-uniformity of shear resistance within interfaces.

As a consequence of the above factors, screw dislocations cross slip from the initial glide planes, which are non-parallel to the interface plane, into the interface with associated core spreading. A single mixed dislocation, from either Cu or Nb, cannot cross the interface even at resolved shear stresses in excess of 1.0 GPa.

Combining atomistic modeling and anisotropic elastic analysis, it was also found that the glide of lattice dislocations in Cu crystal towards the interface is energetically favorable because of the reduction in the line energy of dislocations. For lattice dislocations in Nb gliding towards the interface, the line energy initially increases owing to the Koehler repulsive force. However, the interface shear generates an attractive force that increases with decreasing distance from the interface. Correspondingly, a critical distance exists for lattice glide dislocations in Nb entering the interface. This critical distance is found to be ~1.5 nm. More importantly, this critical distance implies that dislocations cannot be stored within the Nb layer if the thickness of the Nb layer is <3 nm.

## Acknowledgements

This work was supported by the US Department of Energy, Office of Science, Office of Basic Sciences.

## References

[1] Misra A, Verdier A, Lu YC, Kung H, Mitchell TE, Nastasi M, et al. Scripta Mater 1998;39:555.
[2] Clemens BM, Kung H, Barnett SA. MRS Bull 1999;24:20.
[3] Phillips MA, Clemens BM, Nix WD. Acta Mater 2003;51:3157.
[4] Misra A, Hoagland RG, Kung H. Philos Mag 2004;84:1021.
[5] Misra A, Hirth JP, Hoagland RG, Embury JD, Kung H. Acta Mater 2004;52:2387.
[6] Misra A, Hirth JP, Hoagland RG. Acta Mater 2005;53:4817.
[7] Wang YC, Misra A, Hoagland RG. Scripta Mater 2006;54:1593.
[8] Anderson PM, Bingert JF, Misra A, Hirth JP. Acta Mater 2003;51:6059.
[9] Li Z, Anderson PM. Acta Mater 2005;53:1121.
[10] Friedman LH, Chrzan DC. Phys Rev Lett 1998;81:2715.
[11] Fang L, Friedman LH. Philos Mag 2005;85:3321.
[12] Anderson PM, Li C. Nanostruct Mater 1995;5:349.
[13] Rao SI, Hazzledine PM. Philos Mag A 2000;80:2011.
[14] Shen Y, Anderson PM. Acta Mater 2006;54:3941.
[15] Anderson PM, Li Z. Mater Sci Eng A 2001;319:182.
[16] Hoagl RG, Kurtz RJ, Henager CH. Scripta Mater 2004;50:775.
[17] Hoagland RG, Mitchell TE, Hirth JP, Kung H. Philos Mag A 2002;82:643.
[18] Hoagland RG, Hirth JP, Misra A. Philos Mag 2006;86:3537.
[19] Demkowicz MJ, Wang J, Hoagland RG. In: Hirth JP, editor. Dislocations in Solids, vol. 14. Amsterdam: Elsevier; 2008. p. 141. Chap. 83.
[20] Demkowicz MJ, Hoagland RG. J Nucl Mater 2008;372:45.
[21] Wang J, Hoagland RG, Hirth JP, Misra A. Acta Mater 2008;56:3109.
[22] Misra A, Demkowicz MJ, Wang J, Hoagland RG. JOM 2008:39.
[23] Voter AF, Chen SP. Mater Res Soc Symp Proc 1987;82:175.
[24] Johnson RA, Oh DJ. J Mater Res 1989;4:1195.
[25] Liu CL, Cohen JM, Adams JB, Voter AF. Surf Sci 1991;253:334.
[26] Huang H, Wang J. Appl Phys Lett 2003;83:4752.
[27] Wang J, Huang H, Cale TS. Model Simul Mater Sci Eng 2004;12:1209.
[28] Voter AF. In: Westbrook JH, Fleischer RL, editors. Intermetallic Compounds: Principles and Practice, vol. 1. New York: Wiley; 1994. p. 77.
[29] Foiles SM, Baskes MI, Daw MS. Phys Rev B 1986;33:7983.
[30] Voter AF, Chen SP. Mater Res Soc Symp Proc 1987;82:175.
[31] Kaufman L. CALPHAD 1978;2:117.
[32] Kresse G, Joubert D. Phys Rev B 1999;59:1758.
[33] Baskes MI, Srinivasan SG, Valone SM, Hoagland RG. Phys Rev B 2007;75:94113.
[34] Henager CH, Kurtz RJ, Hoagland RG. Philos Mag A 2004;84:2277.
[35] Wang J, Hoagland RG, Misra A. J Mater Res 2008;23:1009.
[36] Barnett DM, Lothe J. J Phys F 1974;4:1618.
[37] Barnett DM, Lothe J, Nishioka K, Asaro RJ. J Phys F 1973;3:1083.
[38] Misra A, Zhang X, Hammon D, Hoagland RG. Acta Mater 2005;53:221.